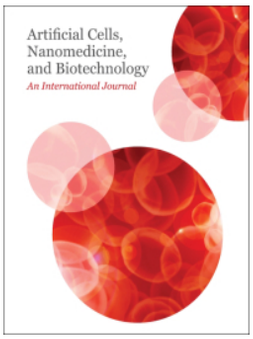

Taylor & Francis
Taylor & Francis Group

Artificial Cells, Nanomedicine, and Biotechnology
An International Journal

ISSN: (Print) (Online) Journal homepage: www.tandfonline.com/journals/ianb20

Antimicrobial capping agents on silver nanoparticles made via green method using natural products from banana plant waste

Jimmy K. Kabeya, Nadège K. Ngombe, Paulin K. Mutwale, Justin B. Safari, Gauta Gold Matlou, Rui W.M. Krause & Christian I. Nkanga

To cite this article: Jimmy K. Kabeya, Nadège K. Ngombe, Paulin K. Mutwale, Justin B. Safari, Gauta Gold Matlou, Rui W.M. Krause & Christian I. Nkanga (2025) Antimicrobial capping agents on silver nanoparticles made via green method using natural products from banana plant waste, Artificial Cells, Nanomedicine, and Biotechnology, 53:1, 29-42, DOI: 10.1080/21691401.2025.2462335

To link to this article: https://doi.org/10.1080/21691401.2025.2462335

Published online: 07 Feb 2025.

ARTIFICIAL CELLS, NANOMEDICINE, AND BIOTECHNOLOGY
2025, VOL. 53, NO. 1, 29–42
https://doi.org/10.1080/21691401.2025.2462335

Antimicrobial capping agents on silver nanoparticles made via green method using natural products from banana plant waste

Jimmy K. Kabeya[a,b,c], Nadège K. Ngombe[a,c], Paulin K. Mutwale[a,c], Justin B. Safari[b,d], Gauta Gold Matlou[e], Rui W.M. Krause[b†] and Christian I. Nkanga[a]

[a]Centre de Recherche en Nanotechnologies Appliquées aux Produits Naturels (CReNAPN), Department of Medicinal Chemistry and Pharmacognosy, Faculty of Pharmaceutical Sciences, University of Kinshasa, Kinshasa XI, Democratic Republic of the Congo; [b]Center of Chemico- and Bio-Medical Research (CCBR), Department of Chemistry, Faculty of Science, Rhodes University, Grahamstown, South Africa; [c]Centre d'Etudes des Substances Naturelles d'Origine Végétale (CESNOV), Medicinal Chemistry and Pharmacognosy, Faculty of Pharmaceutical Sciences, University of Kinshasa, Kinshasa XI, Democratic Republic of the Congo; [d]Department of Pharmacy, Faculty of Pharmaceutical Sciences and Public Health, Official University of Bukavu, Bukavu, Democratic Republic of the Congo; [e]Electron Microscopy Unit, Sefako Makgatho Health Sciences University, Ga-Rankuwa, South Africa

ABSTRACT

Herein, we investigated the phytochemical composition and antibacterial activities of the organic layers from biosynthesized silver nanoparticles (AgNPs). AgNPs were synthesized using *Musa paradisiaca* and *Musa sapientum* extracts. UV-vis absorption in the 400–450 nm range indicated surface plasmonic resonance peak of AgNPs. Samples analyses using dynamic light scattering and transmission electron microscopy revealed the presence of particles within nanometric ranges, with sizes of 30–140 nm and 8–40 nm, respectively. Fourier transform infrared (FTIR) unveiled the presence of several organic functional groups on the surface of AgNPs, indicating the presence of phytochemicals from plant extracts. Thin layer chromatography (TLC) of the phytochemicals (capping agents) from AgNPs identified multiple groups of secondary metabolites. These phytochemical capping agents exhibited antibacterial activities against *Staphylococcus aureus*, *Escherichia coli*, and *Pseudomonas aeruginosa*, with minimum inhibitory concentrations ranging from 62.5 to 1000 µg/mL. Regardless of the bacterial species or plant parts (leaves or pseudo-stems), capping agents from *M. sapientum* nanoparticles displayed significantly enhanced antibacterial effectiveness compared to all other samples, including the raw plant extracts and biosynthesized capped and uncapped AgNPs. These results suggest the presence of antimicrobial phytochemicals on biosynthesized AgNPs, highlighting the promise of green nanoparticle synthesis as a valuable approach in bioprospecting antimicrobial agents.

GRAPHICAL ABSTRACT

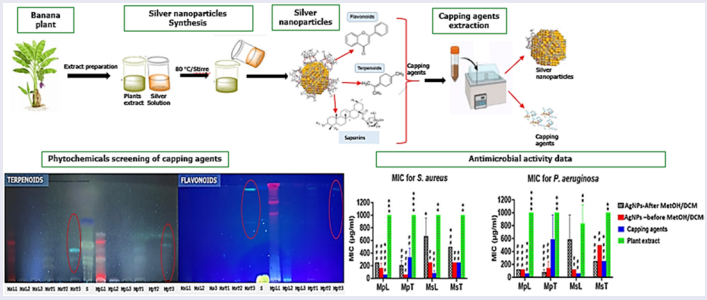

ARTICLE HISTORY

Received 23 August 2024
Revised 12 January 2025
Accepted 29 January 2025

KEYWORDS

Green synthesis; silver nanoparticles; capping agents; antimicrobial activity

CONTACT Christian I. Nkanga christian.nkanga@unikin.ac.cd Centre de Recherche en Nanotechnologies Appliquées aux Produits Naturels (CReNAPN), Department of Medicinal Chemistry and Pharmacognosy, Faculty of Pharmaceutical Sciences, University of Kinshasa, B.P. 212, Kinshasa XI, Democratic Republic of the Congo

†Dedicated in memoriam of Prof. Rui W.M. Krause (1970–2024), a globally recognised leader in Organic Medicinal Chemistry and Nanomaterials, who inspired and nurtured countless young minds to reach their fullest potential.

Introduction

Antimicrobial resistance (AMR) significantly threatens to global public health and economic stability across many countries. According to the World Health Organisation (WHO), AMR is an escalating challenge that gradually complicates the prevention and treatment of infectious diseases [1]. A predictive study in the United Kingdom (UK) has issued a stark warning, estimating that AMR could result in over 10 million annually by 2050 if no effective measures are implemented [2]. Despite the critical need for new antimicrobial agents owing to the alarming rise of AMR, the last three decades have seen a disappointing trickle of new drugs reaching the market, with the most recent class of antibacterial agents discovered in 1980 [3]. This underscores the urgent necessity for innovative drug discovery strategies to combat the rising threat of superbugs. A wish that ties in with The WHO Global Action Plan (2017) to combat antimicrobial resistance, whose Goal 5 highlights the importance of investing in the development of new medicines, diagnostic tools, vaccines and other interventions to combat the emergence and spread of antimicrobial resistance [4].

The discovery of new antimicrobial agents faces challenges partly due to the difficulties in contemporary drug discovery approaches. These include the scarcity of novel targets and the intricate, protracted processes involved in drug development. From the 1980s to 2015, the number of pharmaceutical companies actively investing in antibiotic research dwindled dramatically from 20 to just five highlighting the difficulty and declining investment in this crucial area [3]. This reduction reflects broader systemic issues within the pharmaceutical industry, which hinder the introduction of essential new antimicrobial agents.

Most existing antimicrobial agents are now frequently used in combinations, a strategy employed in a desperate attempt to combat AMR. Exploring medicinal plants as an alternative pathway for discovering new anti-infectious molecules offers a promising avenue to combat harmful microorganisms. Numerous research initiatives around the globe are dedicated to this endeavour, with promising outcomes reported in studies such as those by Porras et al. [5]. These efforts underscore the potential of natural compounds in the ongoing battle against infectious diseases and resistance mechanisms.

Molecular biology, in silico methods, nanotechnology, and other innovative strategies are being harnessed to optimise drug discovery and bring about new antimicrobial molecules from plants [6,7]. Of all these techniques, nanotechnology, particularly green nanotechnology, has captivated the interest of medicinal chemists over the past few decades. Green nanotechnology leverages bio-derived materials, such as plant extracts, to produce antimicrobial metallic nanoparticles (MNPs) [8]. This approach is especially appealing because plant-derived MNPs have shown greater efficacy than MNPs produced by other methods [9].

In a notable study by Nithya et al. the antimicrobial efficacy of chemically synthesised ZnO nanoparticles was compared to ZnO nanoparticles that were synthesised using the plant *Cardiospermum halicacabum*. The results demonstrated that the "green-synthesised" nanoparticles exhibited a more pronounced antimicrobial activities [10]. This finding aligns with numerous other studies that have reported similar outcomes [11]. Importantly, some researchers, have suggested that the presence of organic compounds on the surface of biosynthesized MNPs could be a contributing factor to their enhanced antimicrobial properties [12,13]. The organic compounds surrounding MNPs potentially interact with microbial cells more effectively, thereby boosting the antimicrobial action of the nanoparticles. The environmentally friendly nature of green nanotechnology, coupled with the potent antimicrobial properties of the resulting MNPs, underscores its potential in advancing the field of antimicrobial research.

However, to the best of our knowledge, little is known about the phytochemical composition of the organic compounds surrounding synthesised MNPs. Recent research by Hawadak et al. [14], Fourier Transform Infra-red Spectroscopy (FTIR) was employed to suggest the presence of flavonoids, phytosterols, carbohydrates, proteins, and amino acids on the surface of silver nanoparticles (AgNPs) synthesised from *Azadirachta indica*. However, it's important to note that while FTIR is a valuable tool for detecting functional groups and characterising chemical bonds, it may not be the most reliable method for precisely identifying specific phytochemical compounds from plant materials. The technique's limitations in distinguishing between similar compounds mean that additional analytical methods are often necessary to confirm the presence and structure of specific phytochemicals in such nanoparticles.

Knowing that the organic layer surrounding MNPs synthesised from certain plant extracts has been reported to possess biological properties (antimicrobial, antifungal…) that can add to or potentiate those of the MNPs, we set out to explore ecologically synthesised MNPs as a potential source of bioactive molecules to combat antimicrobial resistance.

Consequently, the current study, therefore, aims to utilise the synthesis of MNPs, using banana plant wastes as raw materials for bioprospecting antimicrobial compounds.

The rationale for selecting banana plant species as the focus of this study is rooted in their environmental and ecological impact. Banana plants produce vast quantities of waste (pseudo stems, leaves, fruit peels…) annually, posing significant environmental threats. According to Mohiuddin et al. several million tons of plant waste are generated each year from global banana plantations [15]. This waste presents a particular challenge in developing countries, where it could be economically repurposed as raw materials for various industries, including biomedical green nanotechnologies. Utilising banana plant waste would not only mitigate its ecological impact but would also promote sustainable practices by providing valuable resources to produce bioactive molecules and greenly synthesised MNPs for myriad biomedical applications, including the fight against antimicrobial resistance. This approach aligns with sustainable development goals and offers potential economic benefits to regions burdened by agricultural waste.

In this work, we prepared and characterised AgNPs; subsequently, we tried to extract the secondary metabolites surrounding these metallic nanoparticles and screened them for

antimicrobial activities and phytochemical composition using thin layer chromatography (TLC).

Materials and methods

Materials

Plants materials

Plant materials samples of banana leaves and pseudo-stems were collected with permission from Centre d'Etudes des Substances Naturelles d'Origine Végétale (CESNOV), University of Kinshasa, and local political authority of the village of Seke Banza located in the province of Kongo Central, DR Congo. Specimens were deposited at the herbarium of the Institut National d'Etudes et de Recherches en Agronomie (INERA) in Kinshasa (DR Congo), and identified by Prof Lukoki Felicien as *Musa sapientum* (voucher specimen no. 001/22) and *Musa paradisiaca* (voucher specimen no. 002/22). Because these two banana species are considered non-protected domesticated plant species by the DR Congo Sustainable Development Department of the National Environment Ministry, under the DR Congo national nature conservation law (Law No. 14/003 of February 11, 2014), only the above-mentioned institutional and local authority permissions were required for their collection. Additionally, the use of these plant materials in the study was granted exemption from the ethical committee of the School of Public Health of the University of Kinshasa, because our research protocol did not involve any biological or human subjects. The plant material was thoroughly washed with distilled water, cut into small pieces, and then dried in an oven at 40 °C for five days before being ground into a fine powder.

Chemicals

All solvents were of analytical grade and purchased from Merck (Germany) and VWR Chemicals Prolabo (Leuven, Belgium). Caffeic acid, gallic acid, rutin, hyperoside and isoquercitrin (HPLC grade) and dimethyl sulfoxide (DMSO) were purchased from Sigma (Bornem, Belgium). Silver nitrate ($AgNO_3$) was purchased from Merck (India). Water was treated in a Milli-Q water ultra-purification system (Dominique DUTSCHER SAS, rue de Bruxelles) before use.

Microbiological materials and culture mediums

In the present study, three different strains of bacteria namely *Staphylococcus aureus* ATCC 29213 (gram-positive), *Escherichia coli* ATCC 25922, and *Pseudomonas aeruginosa* ATCC 25783 (gram-negative) from the American Type Culture Collection (Manassas, VA, USA) were used. The strains were recovered from stocks by cultured overnight at 37 °C under aerobic conditions in Mueller-Hinton from Merck, Darmstadt (Germany).

Methods

Preparation of aqueous extract

The aqueous extract of leaves and pseudo stems of *M. sapientum* and *M. paradisiaca* was used as capping and reducing agent for the synthesis of silver nanoparticles (AgNPs). The preparation of extract was done by decoction as follows: leaves or pseudo stems powder (10 g) was placed in 100 ml of ultrapure water, and then placed on a hot plate at 80 °C for 10 min. The resultant liquid extracts were subsequently filtered by Whatman filter paper (150 mm filter discs, GE Healthcare, UK Ltd) and centrifuged at 3000 rpm for 30 min (U-320 centrifuge, BOECO Germany) to ensure the removal of any macroparticles from plant materials. The resulting filtrate/supernatant was stored at 4 °C for further use as a reducing and stabilising agent [16,17].

Synthesis of silver nanoparticles

The synthesis of AgNPs was performed using the method described by Suresh et al. [18] with slight modifications. Briefly, 50 ml of aqueous plant extract was slowly added to 100 ml of a 10 mM solution of silver nitrate ($AgNO_3$) while under magnetic agitating at 300 rpm and heating at 80 °C for 1 h. The complete bio-reduction of $AgNO_3$ to Ag° ions was confirmed by visual observation of colour change, from dark yellow to dark brown. Subsequently, the colloidal mixture was centrifuged at 13,000 rpm for 10 min at 10 °C and rinsed with ultrapure water three times to remove any impurities and unreacted reagents. AgNPs were then dried in an oven for 24h at 40 °C.

Physicochemical characterisations of silver nanoparticles

UV-Vis spectroscopy. The UV-Vis analysis was done by using a double beam spectrophotometer (Shimadzu UV-2550 spectrophotometer). Some sample AgNPs were suspended in ultrapure water (1 mg/mL), and the suspension was placed at the ultrasonic baths for 1 h to facilitate their dispersion in water. Then filtered using a 0.22 µm syringe filter. The UV-Vis spectrum was obtained using wavelength range of 300–700 nm. Ultrapure water was used as the blank for UV-Vis experiments [19,20].

Particle size analysis and zeta potential measurement by DLS. Particle size analysis was employed to determine the size distribution and the nature of the particle's motion in the medium. Zeta potential is the key parameter to reveal the stability and degree of electrostatic repulsive forces present between similarly charged and adjacent nanoparticles of biosynthesized AgNPs in a colloidal dispersion. This technique relies on tracking the Brownian motion of nanoparticles in solution, which occurs randomly in all directions. Smaller particles move more rapidly than larger ones. As a result, the range of Dynamic Light Scattering (DLS) measurements is constrained to particles as small as 10 nm, since larger particles are too heavy to display significant Brownian motion [21,22]. For the nanoparticles, a high negative zeta potential value confers high dispersity, good colloidal nature, long-term stability, and without aggregation. The high stability of AgNPs is crucial for their biomedical applications [23]. These analyses were observed using a Zetasizer, Nano-ZEN3600 system (Malvern Inc.). The processing of the DLS raw data was performed using the Zetasizer software (Soft Scientific).

FT-IR analysis. FT-IR measurements of AgNPs were taken using a Perkin Elmer Spectrum 100 FT-IR Spectrophotometer.

FTIR spectra were collected in the frequency range of 4000–600 cm^{-1}, and 8 scans were performed for each sample.

Transmission electron microscopy. The transmission electron microscopy (TEM) morphological studies were conducted using JEOL-JEM-1010 electron microscope equipped with the Olympus ITEM TEM imaging platform. The various AgNPs were added to 10 ml of ethanol and sonicated for 2 h to disperse the nanoparticles before dropping on formvar TEM grids for drying.

Phytochemical analysis of AgNPs capping agent by thin layer chromatography (TLC)

TLC was used to analyse the components of the plant extracts and those on the surface of the greenly synthesised nanoparticles. Phytochemicals on the surface of NPs were extracted by maceration in methanol and dichloromethane (10 mg/mL) for 48 h at room temperature. The resultant mixture was then sonicated for 4 h, followed by centrifugation at 4000 rpm for 20 min at 10 °C., and the supernatant was collected for TLC analysis. Each group of metabolites was eluted using a specific solvent system: (i) Ethyl acetate: formic acid, glacial acetic acid, water (100: 11: 11: 26; V/V) for Flavonoids and phenolic acids; (ii) toluene, ethyl acetate (9: 1; V/V) for Terpenoids; (iii) ethyl acetate, formic acid, water (100:10:40; V/V) for Anthocyanins; (iv) ethyl acetate, methanol, water (40:8:5; V/V) for Anthraquinons; (v) dichloromethane, methanol, ammoniac 25% (8: 2: 0,5; V/V) for Alkaloids; (vi) dichloromethane, methanol, water (80: 20: 2; V/V) for Saponins; (vii) ethyl acetate, toluene (10: 93; V/V) for Coumarins [24].

Antimicrobial activities

Antibacterial activity was tested on the plant extracts (decoction) used for green synthesis, on the synthesised AgNPs, on the AgNPs stripped of their organic layer after extraction with a methanol-dichloromethane mixture, and on the methanol-dichloromethane extracts of the organic layer surrounding the AgNPs, from which we removed the solvents by evaporation in an oven.

The minimum inhibitory concentrations (MICs) were determined by standard broth microdilution method based on the clinical and laboratory standards institute (CLSI) guidelines [25,26]; Mueller Hinton broth (Merck, Darmstadt, Germany) was used to determine the MICs for all bacterial strains. Strains were cultured in 96-well microplates. To evaluate the inhibitory effects of the extracts on bacterial growth, each well was supplemented with a range of concentrations (2000, 1500, 1000, 500, 250, 125, and 62.5 µg/mL in 5% DMSO) of the active agents and the experiments were done in triplicate. Following 24 h incubation at 37 °C, the wells were inspected for microbial growth, and the MIC was defined using the resazurin test [27].

Statistical analysis

Data were plotted and statistically analysed using GraphPad Prism 10.1.2. Comparisons were done using one-way analysis of variance (ANOVA) followed by Tukey's multiple comparison test. Asterisks in the figures indicate significant differences with biosynthesized or simply "capped" NPs, (*$p < 0.05$; **$p < 0.01$; ***$p < 0.001$; ****$p < 0.0001$) whereas hashtags

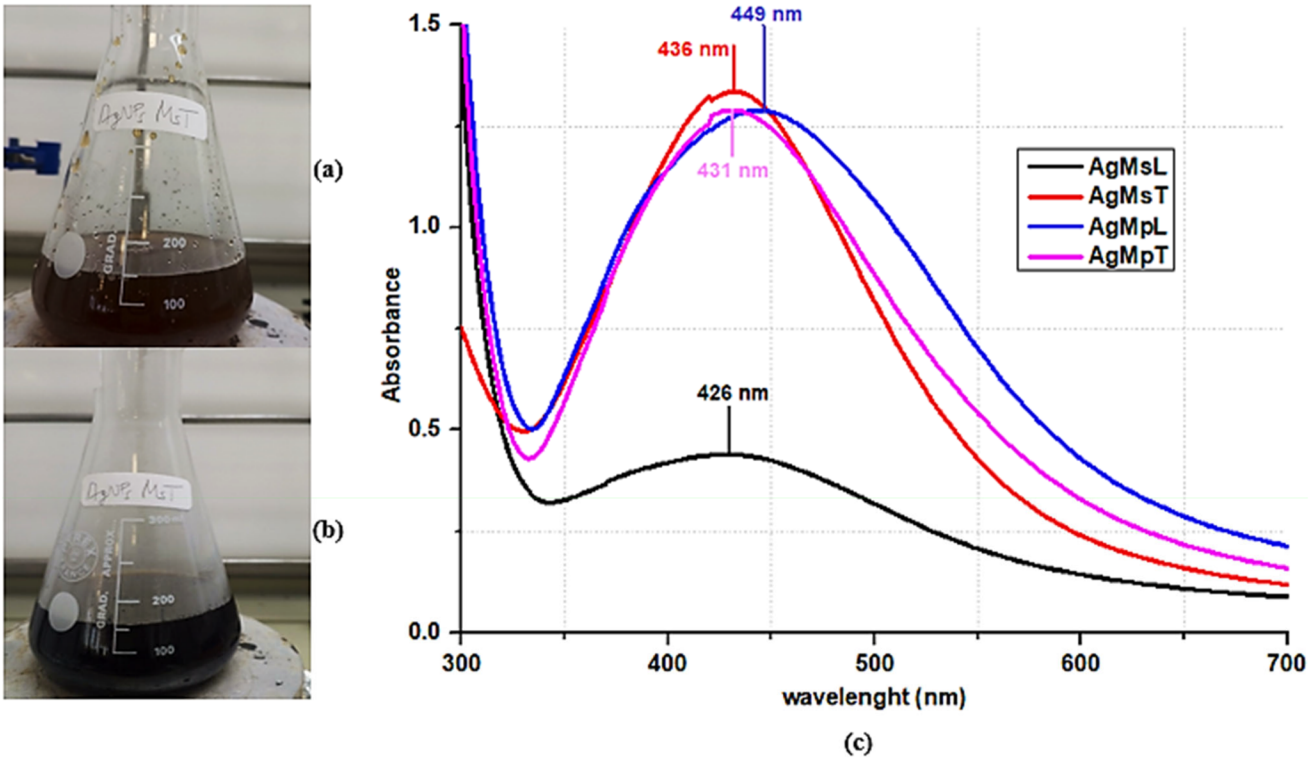

Figure 1. Illustrative data demonstrating AgNPs formation from leaves extract and pseudo stem extract of *M. paradisiaca and M. sapientum;* (a) Visual appearance of reaction mixture, showing colour change from dark yellow before the reaction to dark brown after the reaction (b). (c) UV-vis absorption spectra of AgNPs samples. AgMpL and AgMpT denote AgNPs prepared from the leaves and pseudo stem of *M. paradisiaca*; while AgMsL and AgMsT refer to AgNPs from the leaves and pseudo stem of *M. sapientum*, respectively.

represent significant differences with plant extracts (#$p < 0.05$; ##$p < 0.01$; ###$p < 0.001$; ####$p < 0.0001$).

Results and discussion

Silver nanoparticles synthetised

AgNPs were synthesised using an extract from the leaves and pseudo stems of banana plants (*M. paradisiaca* and *M. sapientum)* combined with a 10 mM solution of silver nitrate. The noticeable colour transition from dark-yellow to dark-brown during the synthesis process indicated the successful reduction of silver ions (Figure 1(a,b)). This colour change serves as a visual confirmation of AgNPs synthesis, reflecting the chemical alterations occurring as the silver ions are reduced and stabilised by the plant extract components as reported by other research [28]. The observed dark-brown colour is attributed to the surface plasmon resonance (SPR) absorption, a phenomenon arising from the collateral vibration of free electrons in metallic silver resonating with the light wave. This SPR property is crucial as it imparts distinctive optical properties to the metallic material arising from the reduction of silver ions [29,30]. As illustrated in (Figure 1(c)), the results of UV-vis absorption spectroscopy confirm this, showing distinct maximum absorption wavelength of 426, 436, 449, and 431 nm for MsL, MsT, MpL, and MpT, respectively. This observation confirms the presence of AgNPs which absorbed in the region of 400–500 nm [13,31]. The visual appearance of the colour change coupled with the SPR bands on the UV-Vis spectra collectively confirm the formation of AgNPs, corroborating observations consistent with previous studies [32]. In order to optimise the weight conditions of nanoparticles synthesis, we weighed quantities of nanoparticles obtained after synthesis (Table 1), taking into account the concentrations of total extracts of plants used, with the aim of understanding whether the concentration of the extracts has a significant impact on the quantity of nanoparticles synthesised; to do this, after preparing the plant extracts, we took 1 ml of each sample, which we dried in an oven at a constant weight, giving us the concentration of phytochemical molecules per mL. The results showed that the MpL extract yielded a large quantity of nanoparticles, so that its initial concentration was high compared with that of other extracts. However, statistically, the distribution of nanoparticle weights was not regular, which suggests that the concentration of the total extract does not have much influence during the synthesis of the Nanoparticles but rather, the concentrations in the extract of the reducing substances (Flavonoids, Saponins, Terpenoids…) which they depend on several intrinsic factors within the plant, such as the plant maturity, the part used, as well as other parameters related to the extraction procedures (time, Temperature…). On the other hand, this analysis gave us an idea of quantities of nanoparticles to be synthesised, based on analyses to be carried out on nanoparticles.

Table 1. Results of AgNPs weights obtained after synthesis.

Sample type	Phytochemical concentration in liquid plant extract	Phytochemical amount in liquid extract volume used for synthesis	Amount of metal salt (AgNO3) in volume used for synthesis	Quantity of dried nanoparticles obtained
MsL	14 mg/mL	700 mg/50 mL	169.87 mg/100 mL	110 mg
MsT	16 mg/mL	800 mg/50 mL	169.87 mg/100 mL	130 mg
MpL	16 mg/mL	800 mg/50mL	169.87 mg/100 mL	410 mg
MpT	12 mg/mL	600 mg/50 mL	169.87 mg/100 mL	116 mg

MsL, total extract from *Musa sapientum* leaves; MsT total extract from *Musa sapientum* pseudo stems MpL extract from *Musa paradisiaca* leaves; MpT extract from *Musa paradisiaca* pseudo stems.

Transmission electron microscopy (TEM)

Morphological characteristics of AgNPs was studied by TEM and showed well-dispersed spherically shaped AgNPs with sizes ranging from 8 to 40 nm (Figure 2). The knowledge of metallic nanoparticles' size and shape is crucial, because these parameters are largely correlated to their biological properties such as antimicrobial and anticarcinogenic activities [33,34]. Indeed, the antibacterial activity of AgNPs is due to their ability to generate Ag + from the oxidative dissolution caused by contact with the bacterial membrane. It was reported that smaller nanoparticles dissolve faster, therefore releasing more Ag + in a short period of time [35,36]. Several physical parameters such as pH and temperature have shown remarkable influence on the size and shape of metallic nanoparticles, but other parameters, such as plant compounds that help to reduce metal ions and stabilise nanoparticles, can also have a significant influence [21]. TEM results of our samples are comparable to data reported elsewhere [37,38]. Moreover, TEM analysis allowed us to picture out phytochemicals surrounding AgNPs; the presence of the phytochemical organic matter on the surface of AgNPs were elucidated by amorphous material surrounding the nanoparticles on TEM images. Figure 2 illustrates the high presence of organic materials on AgNPs before MetOH/DCM extraction (AgMpL, AgMsL, AgMpT, and AgMsT), as compared to the low occurring organic material on AgNPs after MetOH/DCM extraction (AgMpLun, AgMsLun, AgMsTun, and AgMpTun); interestingly, even their sizes appeared slightly different (Table 2, Figure 2).

Dynamic light scattering (DLS) measurement

Particles size and particle size distribution profile were investigated using dynamic light scattering (DLS), by studying 50 µg/mL samples at room temperature. DLS hydrodynamic sizes appeared to be larger than TEM sizes, which has been previously reported elsewhere [39,40]. This is caused by DLS sensitivity, which tends to be skewed to larger sizes. All samples showed average distribution sizes ranging from 30 to 140 nm, and a polydispersity index ranged from 0.466 ± 0.06 to 0.447 ± 0.04 (Figure 3, Table 3). Based on the PDI values and size distribution by number graphs, it appears that all samples exhibit nanoparticles that are relatively well dispersed [41]. Furthermore, given all samples confirmed the presence of nanoparticles, DLS data suggests that extracts of different banana plant species have not only good reducing properties, but also good amount of capping agents suitable for obtaining well-dispersed nanoparticles [42]. As shown in Table 3, the zeta potential values were -5.74 ± 90.1 mV for AgMsL; -1.52 ± 38.7 mV for AgMsT; -51.1 ± 79.7 mV for AgMpL;

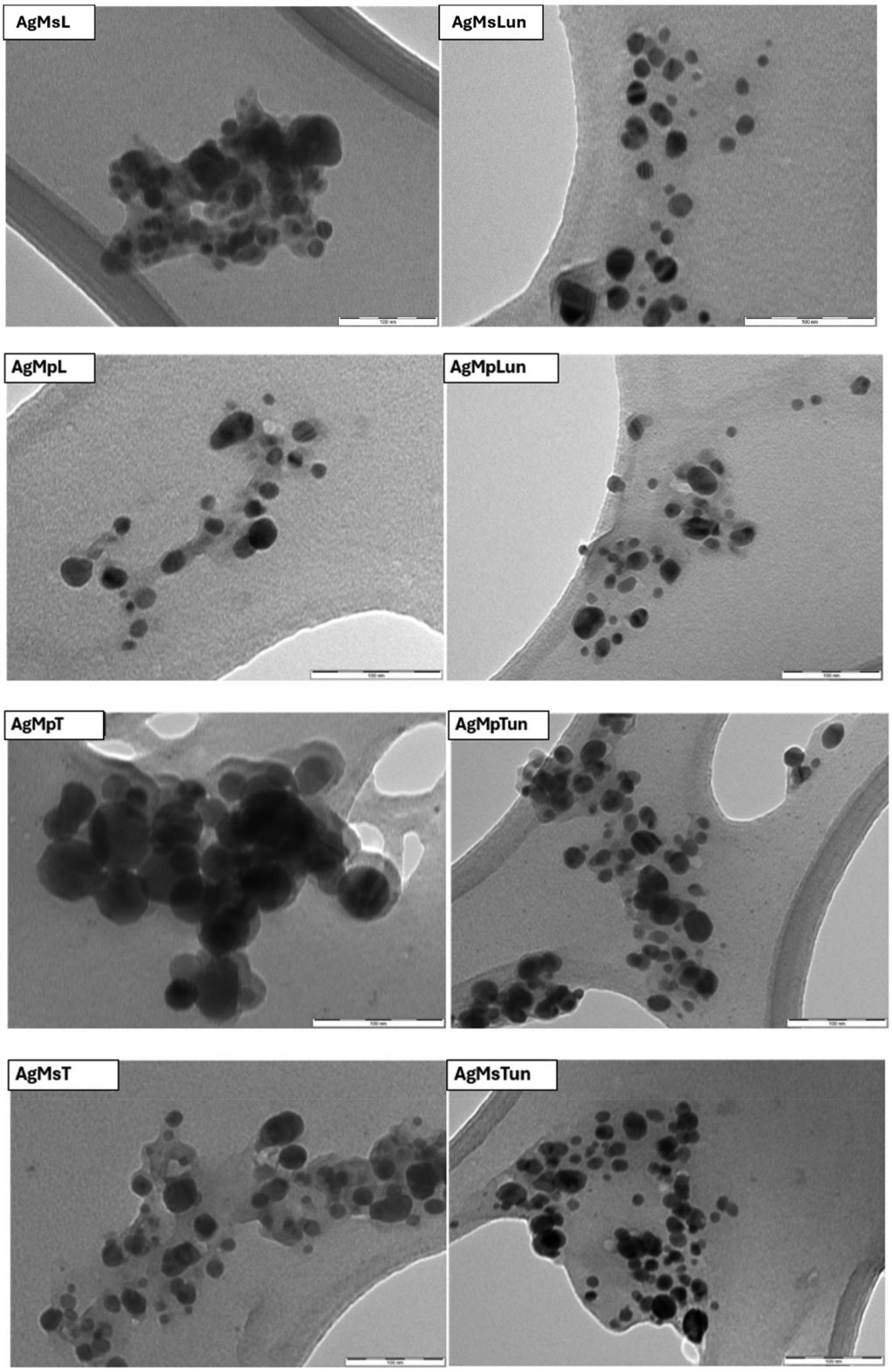

Figure 2. TEM images of AgNPs-before MetOH/DCM extraction (AgMsL, AgMpL, AgMpT and AgMsT) and AgNPs-after MetOH/DCM (AgMsLun, AgMpLun, AgMpTun and AgMsTun). The TEM grid used was coated with formvar as support to allow easy analysis of the nanoparticles. Magnification: 400 000X: Scale: 100 nm.

and −3.29 ± 32.3 mV for AgMpT. Some of the samples exhibited relatively negative values, indicating underlying good stability due to strong electrostatic repulsion between particles, preventing nanoparticle aggregation [43]. This appears to be an asset because zeta potential has a significant influence on the antibacterial activity of nanoparticles. This is explained by the electrostatic interactions between the nanoparticle surface charge and the surface charge of the bacterial cell membrane. When the bacterial membrane is negatively charged, positively charged nanoparticles are more likely to adhere to the surface. Conversely, when the membrane carries a positive charge, negatively charged

nanoparticles tend to get adsorbed onto it [44]. FTIR analysis suggests that this negative charge is likely associated with various negatively charged functional groups (OH, COO, and CH) present on the surface of the AgNPs [45]. These molecular traits confirm the successful synthesis of stable AgNPs with a relatively narrow size distribution.

FTIR spectroscopy

The FTIR spectroscopy analysis was studied to highlight the possible presence phytochemicals compounds surrounding metal nanoparticles during synthesis. Figure 4 presents the FTIR spectra of the AgNPs synthesised using MpL, MpT, MsL, and MsT extracts.

For AgMpL broader bands observed at 3274 cm^{-1} is attributed to the (N–H) bonds stretching, indicating presence of amines compounds. Bands around 2916 cm^{-1} and 2846 cm^{-1} reflect (C–H) alkanes bond stretching. The band of 2113 cm^{-1} shows the presence of alkynes function (C≡C), bands around 1630 cm^{-1} (C=C) Alkenes, 1518 cm^{-1} (N-O) nitro compounds, 1379 cm^{-1} shows (C–H) stretching, 1228 cm^{-1} (C-N) amines, 1060 cm^{-1} (C–O) alcohols, ethers, esters, carboxylic acids; For AgMpT, spectrum shows bands at 3689 and 3619 cm^{-1} indicates the presence of aromatic alcoholic and phenolic compounds, the band at 2993 cm^{-1} indicates the presence stretching vibration bands of (C–H) alkanes, the band at 1624 cm^{-1} is due to the (C=C) unsaturated stretching, the band at 1330 cm^{-1} indicates the presence of (C-H) Alkanes, 1314 cm^{-1} (C-H) Alkanes, 1029 cm^{-1}(O–H) alcohols, ethers, esters, carboxylic acids 780 cm^{-1} (C–H) out-of-plane bending (aromatics) [46].

Same way analysis for AgMsL sample several stretching vibration bands shows at around 3267 cm^{-1}, (N-H) amines, 2918 cm^{-1} (C–H) alkanes, 2850 cm^{-1} (C–H) alkanes, 2120 cm^{-1} (C≡C) alkynes, 1631 cm^{-1} (C=C) Alkenes, 1525 cm^{-1} (N-O) nitro compounds, 1378 cm^{-1} (C–H) methyl groups, 1230 cm^{-1} (C-N) amines, 1029 cm^{-1} (C–O) alcohols, ethers, esters, carboxylic acids, 612 cm^{-1} (C–Cl) Alkyl halides; AgMsT sample, several stretching vibration bands shows at around 2917 cm^{-1} (C–H) alkanes, 2120 cm^{-1} (C≡C) alkynes, 1611 cm^{-1} (C=C) aromatics, 1314 cm^{-1} (C–H) alkanes, 1025 cm^{-1} (O–H) alcohols, ethers, esters, carboxylic acids, 779 cm^{-1} (C–H) out-of-plane bending (aromatics). These results show the presence of functional groups around metal nanoparticles such as alcohols (carboxylic acids), amines, aliphatic chains, carbon structures with multiple bonds, carbonyl groups (acid) and aromatic rings. This, together with the knowledge of *Musa* metabolites leads us to presume the presence of major plant secondary

Table 2. Size variations of AgNPs (TEM).

Type samples	Size range (nm)	Average ± SD (nm)
AgMpL	11.71–25.65	17.18 ± 4.13
AgMpLun	8.58–20.13	13.56 ± 4.21
AgMpT	13.70–41.09	26.03 ± 8.72
AgMpTun	14.16–30.37	21.17 ± 5.05
AgMsL	10.89–21.12	15.84 ± 3.50
AgMsLun	7.97–22.17	14.18 ± 4.25
AgMsT	14.52–29.38	20.51 ± 3.49
AgMsTun	9.24–23.43	17.42 ± 4.03

AgMpL denote AgNPs before MetOH/DCM extraction, prepared from leaves of *M. paradisiaca*, AgMpLun denote AgMpL after extraction; AgMpT denote AgNPs before MetOH/DCM extraction, prepared from the Pseudo stems of *M. paradisiaca*, AgMpTun denote AgMpT after extraction, AgMsL denote AgNPs before MetOH/DCM extraction, prepared from the leaves of *M. sapientum*, AgMsLun denote AgMsL after extraction, AgMsT denote before MetOH/DCM extraction, prepared from the pseudo stems of *M. sapientum*, AgMsTun denote AgMsT after MetOH/DCM extraction.

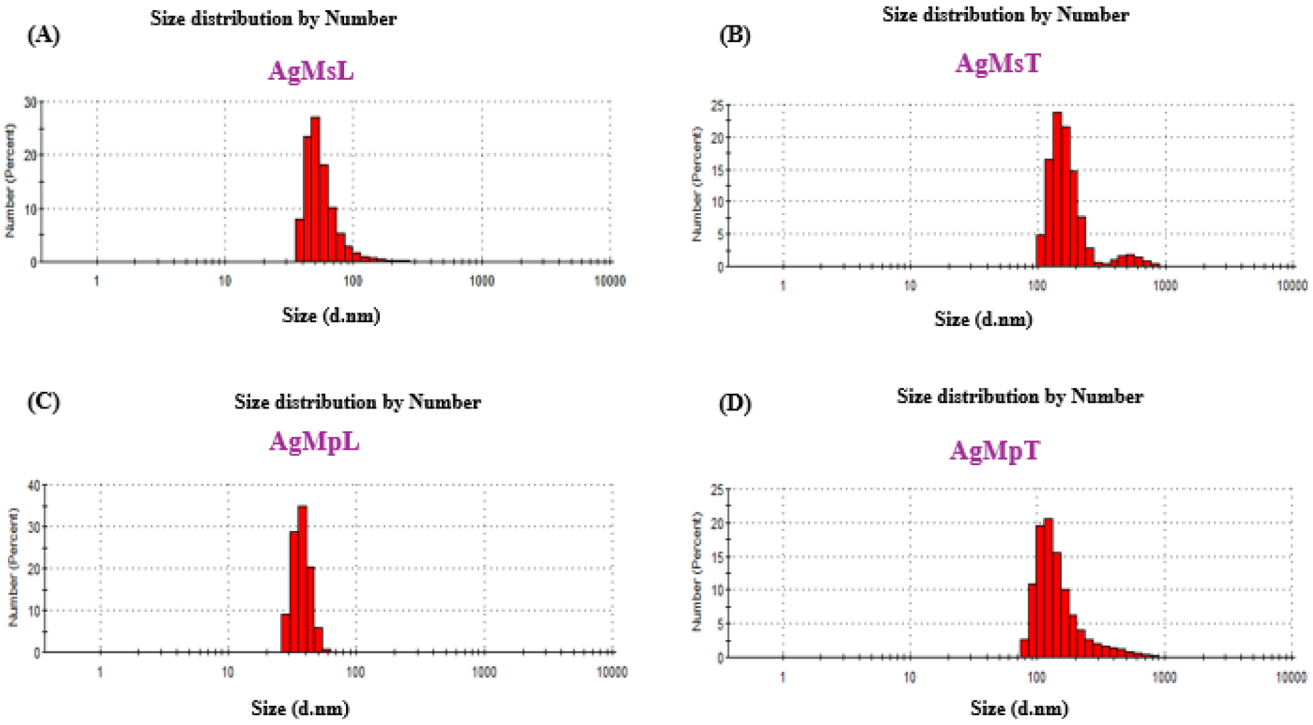

Figure 3. Size distribution by number of AgNPs by DLS. AgMsL (A) and AgMsT (B) denotes AgNPs from the leaves and pseudo stem of *M. sapientum*; AgMpL (C) and AgMpT (D) refers to AgNPs prepared from the leaves and pseudo stem of *M. paradisiaca* respectively.

metabolites on the surface of nanoparticles, such as Terpenoids, Flavonoids, Saponins, Coumarins…; the phytochemical screening results that we have performed have demonstrated this. These results corroborate other researchers who assume the participation of organic compounds of plant origin in potentiating the biological properties of certain nanoparticles [13,47,48]. Moreover, these characteristic functional groups play a crucial role in reducing metal ions into NPs and stabilising them afterward [13,49]. For instance, gallic acid, a type of flavonoid, contains a hydroxyl group (-OH) attached to an aromatic ring. This hydroxyl group exhibits a strong metal-reducing activity, forming an intermediate complex during reduction process, which is subsequently oxidised to quinones. These quinones are believed to remain on the nanoparticles surface, preventing aggregation and ensuring prolonged stability [49,50]. On the other hand, we have observed that spectra of AgMsL and AgMsT samples are similar, whereas spectra of AgMpL and AgMpT are different; this may be due to the difference in phytochemical compounds on the surface of silver nanoparticles. This leads us to believe that depending on the maturity and the part of the plant used to prepare extracts, the phytochemical compound composition is different.

Satisfied of the presence of organic compounds on silver nanoparticles layer, we tried to find out if it was possible to extract this organic layer. we placed the AgNPs in the methanol/dichloromethane mixture (1:1) for 24h at room temperature and then at the ultrasonic baths for 4h, in order to identify them by phytochemical screening and evaluate their biological activities. After extraction, we performed an FTIR spectroscopic analysis to observe whether the extraction was effective. Analysis of results obtained in which we compared the FTIR spectra of the plant extract used for nanoparticle synthesis, capped silver nanoparticles, and silver nanoparticles subjected to extraction of the organic layer (Figure 5) revealed to us that although the extraction of the organic layer by our method was not optimal, we were able to extract a part of this organic layer which we tried to identify by TLC.

Table 3. Particle size and zeta potential of AgNPs (DLS).

Type samples	PS ± SD (nm) ($n=3$)	PDI ± SD ($n=3$)	ZP ± SD (mV) ($n=3$)
AgMpL	37 ± 6	0.466 ± 0.06	−51.1 ± 79.7
AgMpT	91 ± 94	0.431 ± 0.07	−3.29 ± 32.3
AgMsL	58 ± 28	0.44 ± 0.04	−5.74 ± 90.1
AgMsT	91 ± 24	0.447 ± 0.04	−1.51 ± 38.7

PS: particle size, SD: standard deviation, PDI: polydispersity index, ZP: Zeta potential, mV: millivolt, n: number of replicates; AgMsL and AgMsT denotes AgNPs from leaves and pseudo stems of *M. sapientum*; AgMpL and AgMpT refers to AgNPs prepared from leaves and pseudo stems of *M. paradisiaca* respectively.

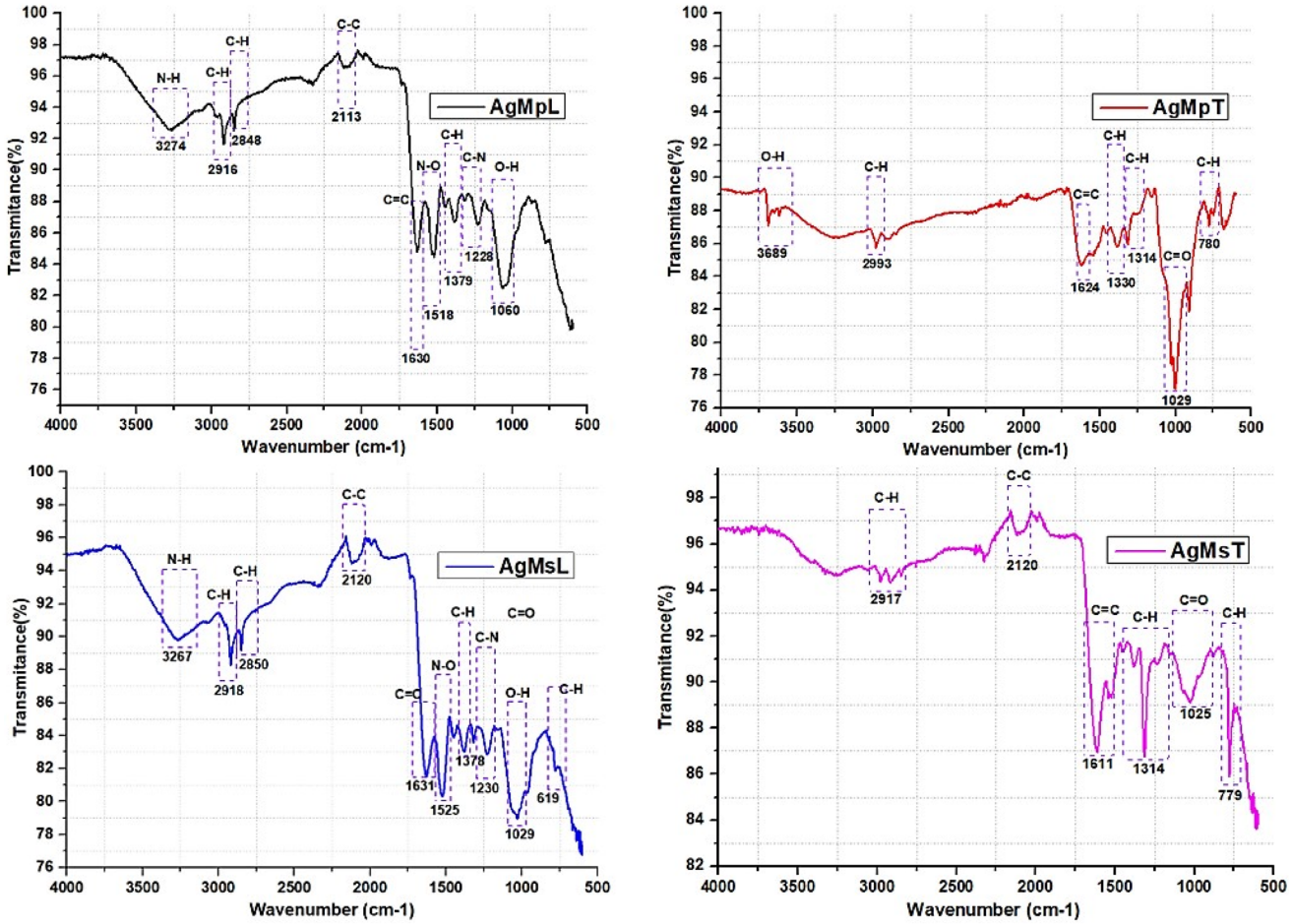

Figure 4. FTIR spectra of AgNPs. AgMpL and AgMpT denote AgNPs prepared from the leaves and pseudo stem of *M. paradisiaca*; while AgMsL and AgMsT refer to AgNPs from the leaves and pseudo stem of *M. sapientum*, respectively.

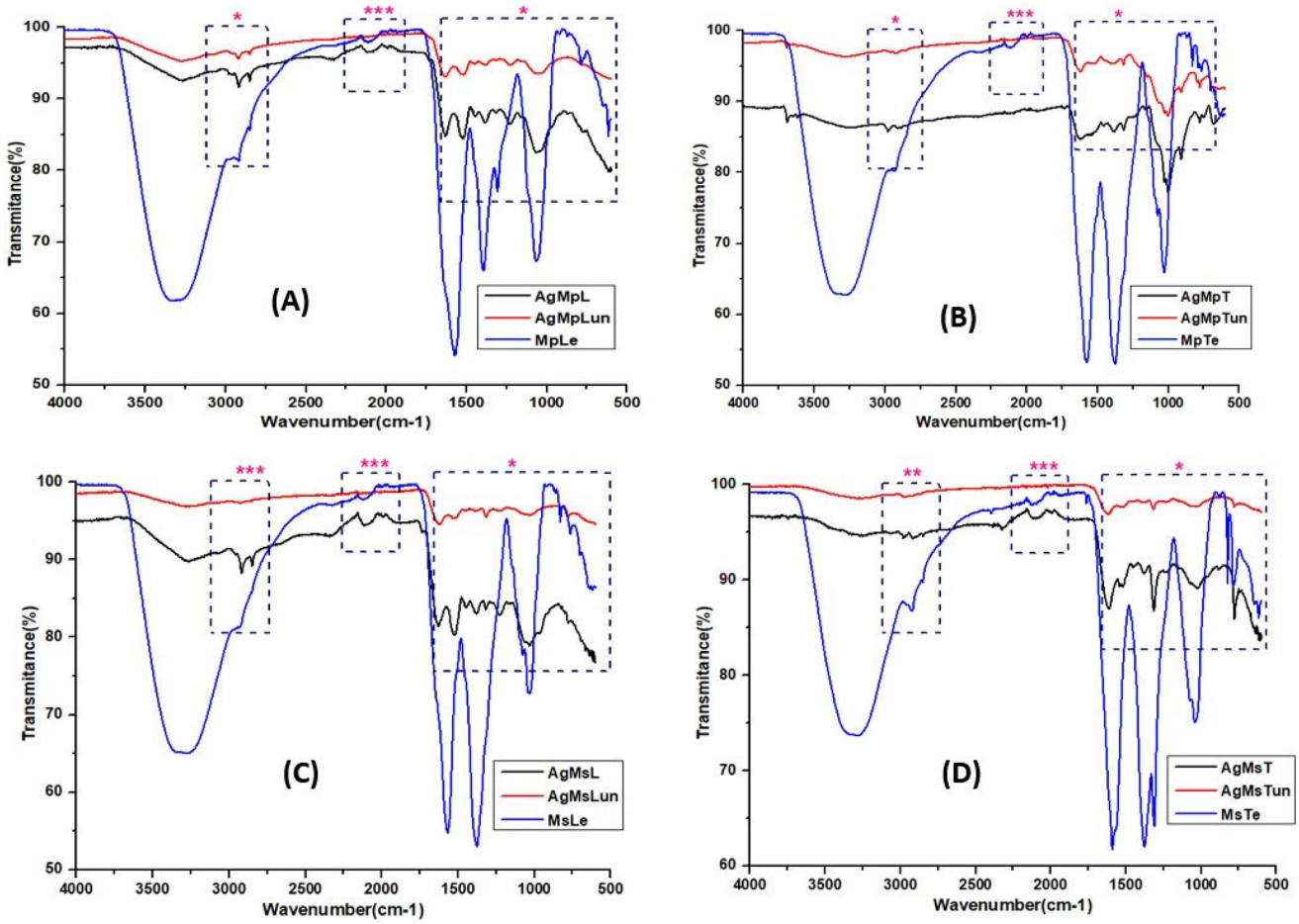

Figure 5. Comparative FTIR spectra of AgNPs between AgNPs before and after methanol /dichloromethane (MetOH/DCM) extraction, and their respective extracts. (A) AgMpL denote AgNPs before MetOH/DCM extraction, prepared from the leaves of *M. paradisiaca*, AgMpLun denote AgMpL after extraction, MpLe denote extract of *M. paradisiaca* leaves; (B) AgMpT denote AgNPs before MetOH/DCM extraction, prepared from the pseudo stems of *M. paradisiaca*, AgMpTun denote AgMpT after extraction, MpTe denote extract of *M. paradisiaca* pseudo stems; (C) AgMsL denote AgNPs before MetOH/DCM extraction, prepared from the leaves of *M. sapientum,* AgMsLun denote AgMsL after extraction, MsLe denote extract of *M. sapientum* leaves; (D) AgMsT denote before MetOH/DCM extraction, prepared from the pseudo stems of *M. sapientum*, AgMsTun denote AgMsT after MetOH/DCM extraction, MsTe denote extract of *M. sapientum* pseudo stems. Asterisks indicate potential extent of extraction: *low extent of extraction; **Middle extent of extraction; ***high extent of extraction.

Phytochemical analysis

Thin layer chromatography (TLC) was employed to analyse the phytochemical compositions of the organic layers extracted from AgNPs, in comparison to the total plant extracts used for the green synthesis (Figure 6 and Table 4). This method allowed for the direct visual comparison of the presence and diversity of phytochemicals in both nanoparticles and the original plant extracts. By separating the various compounds based on their solubility and adsorption characteristics, TLC provides insights into the specific secondary metabolites that are retained or preferentially adsorbed onto the nanoparticle surfaces during green synthesis. This approach is crucial for understanding how the synthesis process may alter or enhance the phytochemical profile of the final nanoparticle product.

The results of phytochemical screening are presented in Table 4 provides a detailed comparison of the phytochemical compositions of the organic compounds capping the nanoparticles and the initial total extracts from plants. Notably, while the starting plant extracts generally contain a broad spectrum of the phytochemical groups, the organic compounds extracted from the corresponding biogenic AgNPs exhibited quite limited and varied phytochemical compositions. The analysis of methanolic extracts from biogenic AgNPs showed the presence of flavonoids across all samples. Interestingly, the capping agents extract labelled "AgMpL", a derivative of AgNPs from *M. paradisiaca* leaves, was found to contain the most comprehensive range of the phytochemical groups investigated, surpassing other AgNPs extracts in secondary metabolites diversity, and displaying almost all the phytochemicals from the corresponding plant extract (as illustrated in Figure 6 and Table 4). This indicates a selective adsorption or bonding of certain phytochemicals onto the AgNPs surfaces during the green synthesis process, which may influence the functional properties of biogenic AgNPs.

These results effectively demonstrate that the synthesis nanoparticles using plant extracts results in the adsorption of plant metabolites onto the nanoparticles, a process that varies depending on the plant species and the specific parts used. This finding is supported by Pereira et al. [51], who observed that extracts from different parts of *Handroanthus heptaphyllus* plant produce AgNPs with distinct physicochemical features. The presence of phytochemicals on nanoparticles synthesised

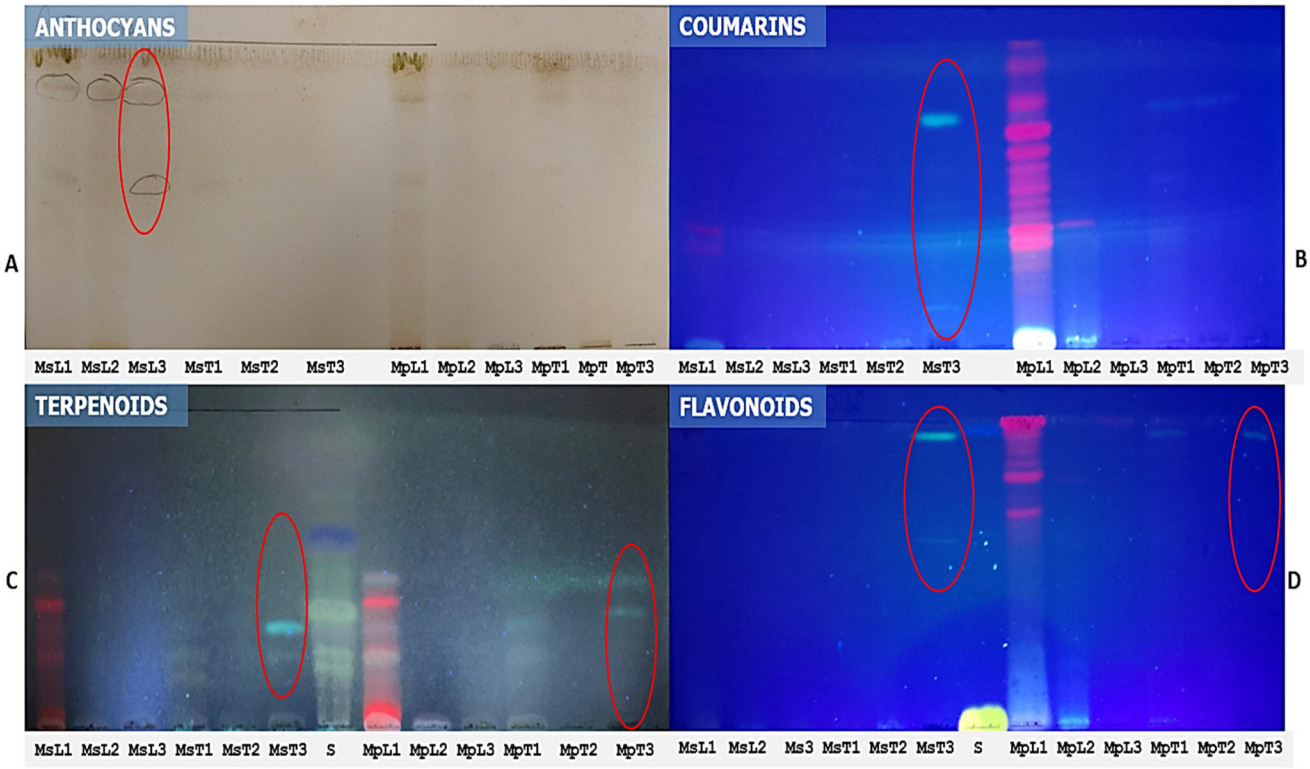

Figure 6. Representative TLC chromatograms of selected secondary metabolites screened from methanolic/dichloromethane (1:1) plant extracts versus aqueous total plant extracts (decoction) versus methanolic/dichloromethane (1:1) AgNPs extracts. (A) TLC plate for Anthocyanins. (B)TLC plate for Coumarins. (C) TLC plate for Terpenoids. (D) TLC plate for flavonoids. MsL1 denotates methanolic/dichloromethane (1:1) extract from *M. sapientum* leaves; MsL2 denotates decoction from *M. sapientum leaves*; MsL3 denotates methanolic/dichloromethane (1:1) extract of AgNPs from *M.* sapientum leaves decoction. MsT1 denotates methanolic/dichloromethane (1:1) extract from *M. sapientum* pseudo stems; MsL2 denotates decoction from *M. sapientum* pseudo stems, MsL3 denotates methanolic/dichloromethane (1:1) extract of AgNPs from *M. sapientum* pseudo stems decoction. MpL1 denotates methanolic/dichloromethan (1:1) extract from *M. paradisiaca* leaves, MpL2 denotates decoction from *M. paradisiaca* leaves, MpL3 denotates methanolic/dichloromethane (1:1) extract of AgNPs from *M. paradisiaca* leaves decoction. MpT1 denotates methanolic/dichloromethane (1:1) extract from *M. paradisiaca* pseudo stems, MpT2 denotates decoction from *M. paradisiaca* pseudo stems, MpT3 denotates methanolic/dichloromethane (1:1) extract of AgNPs from *M. paradisiaca* pseudo stems decoction.

Table 4. Results of phytochemical screening of extracts from plant and biogenic AgNPs using TLC.

Phytochemical compounds	Extract types							
	MsL	AgMsL	MsT	AgMsT	MpL	AgMpL	MpT	AgMpT
Flavonoids	+	–	+	+	+	–	+	+
Terpenoids	+	–	+	+	+	–	+	+
Anthocyanins	+	+	+	–	+	–	+	–
Coumarins	+	+	+	+	+	–	+	–

"+" indicates presence and "–" indicates absent.
MsL, total extract from *Musa sapientum* leaves; AgMsL extract from silver nanoparticles biosynthesized from *Musa sapientum* leaves; MsT total extract from *Musa sapientum* pseudo stems, AgMsT extract from silver nanoparticles biosynthesized from *Musa sapientum* pseudo stems, MpL extract from *Musa paradisiaca* leaves; AgMpL extract from silver nanoparticles biosynthesized from *Musa paradisiaca* leaves; AgMpT extract from silver nanoparticles biosynthesized from *Musa paradisiaca* Pseudo stems.

from plant extracts is crucial, as it contributes to the enhancement of the biological properties of nanoparticles [13,16]. This suggests that systematic selection of plant sources and parts for nanoparticle green synthesis can be strategically used to develop nanoparticles with specific, potent biological activities.

Antimicrobial activity

The antibacterial efficacy of extracts from plants and the organic layers (capping agents) of AgNPs was assessed against *E. coli*, *P. aeruginosa*, and *S. aureus* by determining the minimum inhibitory concentrations (MICs). Figure 7 presents compelling data indicating that all tested bacterial strains were susceptible to the sample extracts, with MICs ranging between 62.5 and 1000 µg/mL. Statistical analysis confirms that phytochemicals ("capping agents") from *M. sapientum* nanoparticles displayed significantly antibacterial activities compared to their counterparts, including crude plant extracts and biogenic AgNPs, regardless of the bacterial species or parts of the plant used. This suggests an augmented antibacterial effect due to the phytochemicals associated with AgNPs, possibly resulting from a concentration increase of bioactive compounds. This finding aligns with previous research indicating that plant phytochemicals can enhance the antibacterial activity of biogenic AgNPs [52].

Based on the FTIR spectra results, the enhanced antibacterial activity of AgNPs may be attributed to the presence of hydroxyl (OH) functional groups from flavonoids found in banana plants [53]. These functional groups are known to interact with the lipid bilayer of the bacterial cell membrane, triggering an oxidative burst that generates reactive oxygen species (ROS). This oxidative stress alters membrane permeability, leading to damage to the bacterial membrane [54,55]. Additionally, the antibacterial properties of silver, particularly in nanoparticle form, are well-documented. AgNPs are believed to disrupt membrane permeability due to their

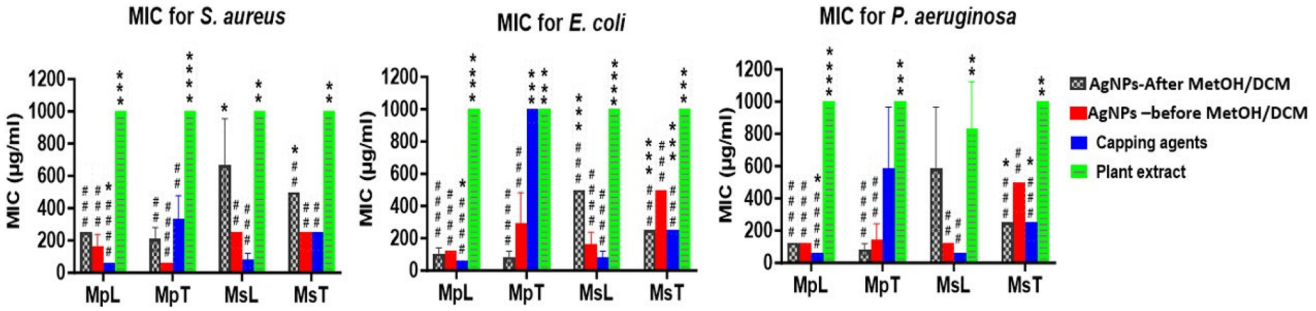

Figure 7. Antimicrobial activity data presenting the minimum inhibitory concentrations (MIC) of extracts from plants and AgNPs with organic layers and AgNPs after methanol and dichloromethane treatment. Herein, "capping agents" refers to the phytochemical extracted from AgNPs synthesised from *M. paradisiaca*'s leaves and pseudo stem (MpL and MpT, respectively) or AgNPs from *M. sapientum*'s leaves and pseudo stem (MsL and MsT, respectively). "AgNPs-before MetOH/DCM" refers to the nanoparticles before methanol/dichloromethane extraction "AgNPs-after MetOH/DCM" refers to the nanoparticles that have been subject to extraction test with methanol and dichloromethane to produce "capping agents" (the phytochemicals surrounding AgNPs). Data were compared using one-way ANOVA followed by tukey's multiple comparison test. #comparison with capped NPs (#p-value < 0.05; ##p < 0.01; ###p < 0.001; ####p < 0.0001). *Comparison with plant extracts (*p-value < 0.05; **p < 0.01; ***p < 0.001; ****p < 0.0001).

capacity of perturbing the bacterial membrane owing to the generation of Ag^+ from the oxidative dissolution, and to their high affinity for sulphur atom. Once inside the cell, Ag + ions bind to proteins containing cysteine and methionine residues, impairing the permeability of the cytoplasmic membrane and compromising the bacterial envelope. This interaction inactivates essential bacterial enzymes, disrupts DNA, and interferes with ribosomal function, thereby inhibiting protein synthesis [35,56].

Interestingly, the capping agents extracted from AgNPs of *M. paradisiaca*'s leaves, which showed the highest number of phytochemicals on TLC, consistently exhibited the lowest MICs. This was a significant deviation from the results of both the crude plant extract and biogenic AgNPs counterparts, across all bacterial species tested. Given the similarity in phytochemical composition between the extracts from the *M. paradisiaca's* leaves and the corresponding AgNPs, the exceptional performance of the capping agents suggests a potential enhancement. This enhancement could be due to molecular modifications of the metabolites when attached to the AgNPs during green synthesis, which underlines the need to identify the molecular structures of the said capping agents to establish whether their phytochemical or artefact origins.

Conclusion

The study aimed to elucidate the phytochemical composition of the organic layers surrounding metallic silver nanoparticle synthesised using banana plant extracts, and assess their biological activities, with a focus on antibacterial effects. After synthesis and characterisation, results obtained from TLC analysis revealed the presence of various phytochemical groups in the organic layers of AgNPs, such as Flavonoids, Terpenoids, Anthocyanins, and Coumarins. Antibacterial analyses using different extracts against three bacterial strains (*S. aureus*, *E. coli*, and *P. aeruginosa*) showed that all extracts notably inhibited the growth of these species, with MICs ranging from 62.5 to 1000 µg/mL. We also observed that the AgNPs derived from *M. sapientum* exhibited stronger antibacterial activity compared to those derived from *M. paradisiaca*. This enhanced activity may be attributed to the richer phytochemical profile of *M. sapientum*. The variance in MICs among the extracts further sparked interest in understanding which the metallic nanoparticles preferentially adsorbed phytochemical groups during synthesis these groups evidently depend on the plant's nature, as reflected by the differing MICs according to the type of plant extract utilised for nanoparticle synthesis. This investigation corroborates the results of phytochemical screenings, which showed a heterogeneous distribution of phytochemical groups among the nanoparticles' capping agents, influenced by the plant species and the part used. Considering these findings, it would be advantageous to conduct comprehensive studies to isolate and identify the molecular species preferentially captured by metallic nanoparticles and examine the specific mechanisms of their capture through green synthesis. Moreover, the extraction used did not completely extract the organic layer from the nanoparticles. Therefore, it is relevant to explore and optimise other extraction methods such as mechanochemistry or other alternative solvent systems like ethanol, acetone, or supercritical CO2. This study's outcome suggest that green nanoparticle synthesis is a promising avenue for the bioprospecting new bioactive molecules with potential applications in antimicrobial treatments.

Acknowledgements

Thank you to the Rhodes University Biopharmaceutics Research Group for the collection of DLS data.

Ethics statement

According to the Ethical Committee of the School of Public Health at the University of Kinshasa (local committee) and European Union regulations, ethical approval from an institutional board was not required for this study. This determination was based on the fact that the research protocol did not involve biological or human subjects. Additionally, under our national nature conservation law, the plant species used in this study are classified as non-protected and domesticated.

The plant materials were collected with institutional authorisation from the Centre d'Etudes des Substances Naturelles d'Origine Végétale (CESNOV) at the University of Kinshasa, Democratic Republic of the

Congo. Furthermore, permission for plant harvesting was obtained from the local political authority of the village of Seke Banza, located in the province of Kongo Central, DR Congo.

Author contributions

JKK: conceptualisation, data curation, investigation, methodology, project administration, software, visualisation and writing original draft. JBS: methodology, software, writing original draft. RWK, PKM, and NKN: validation, supervision, writing-review and editing. CIN: conceptualisation, funding acquisition, methodology, validation, supervision, writing-review and Editing. All the authors reviewed and edited the manuscript. GGM: data curation, technique and characterisation, writing-review and editing.

Disclosure statement

No potential conflict of interest was reported by the authors.

Funding

This document has been produced with the financial assistance of the European Union (Grant no. DCI-PANAF/2020/420-028), through the African Research Initiative for Scientific Excellence (ARISE), pilot program. ARISE is implemented by the African Academy of Sciences with support from the European Commission and the African Union Commission. The contents of this document are the sole responsibility of the authors and can under no circumstances be regarded as reflecting the position of the European Union, the African Academy of Sciences, and the African Union Commission. Thank you to the NRF UIF141979 grant for additional support.

ORCID

Jimmy K. Kabeya http://orcid.org/0000-0003-1463-9422
Nadège K. Ngombe http://orcid.org/0000-0002-2859-7238
Paulin K. Mutwale http://orcid.org/0000-0003-2946-4047
Justin B. Safari http://orcid.org/0000-0002-8940-9552
Gauta Gold Matlou http://orcid.org/0000-0002-2373-2365
Rui W.M. Krause http://orcid.org/0000-0001-6788-6449
Christian I. Nkanga http://orcid.org/0000-0001-7712-478X

Data availability statement

Data are available under: Kabeya Jimmy (2024), "Antimicrobial capping agents on silver nanoparticles made *via* green method using natural products from banana plant waste", Mendeley Data, V1, doi: 10.17632/sfnp4zvkmv.1. Or under this link: https://data.mendeley.com/datasets/sfnp4zvkmv/1

References

[1] Migliori GB, Sotgiu G, Rosales-Klintz S, et al. ERS/ECDC statement: European Union standards for tuberculosis care, 2017 update. Eur Respir J. 2018;51(5):1702678. doi: 10.1183/13993003.02678-2017.
[2] de Kraker MEA, Stewardson AJ, Harbarth S. Will 10 million people die a year due to antimicrobial resistance by 2050? PLOS Med. 2016;13(11):e1002184. doi: 10.1371/journal.pmed.1002184.
[3] Blaskovich MAT, Butler MS, Cooper MA. Polishing the tarnished silver bullet: the quest for new antibiotics. Essays Biochem. 2017;61(1):103–114. doi: 10.1042/EBC20160077.
[4] OMS. Global action plan on antimicrobial resistance. Geneva, Switzerland: World Health Organization; 2017. p. 1–28.
[5] Porras G, Lyles JT, Marquez L, et al. Ethnobotany and the role of plant natural products in antibiotic drug discovery. Chem Rev. 2021;121(6):3495–3560. doi: 10.1021/acs.chemrev.0c00922.
[6] Ejalonibu MA, Ogundare SA, Elrashedy AA, et al. Drug discovery for *Mycobacterium tuberculosis* using structure-based computer-aided drug design approach. Int J Mol Sci. 2021;22(24):13259. doi: 10.3390/ijms222413259.
[7] Privalsky TM, Soohoo AM, Wang J, et al. Prospects for antibacterial discovery and development. J Am Chem Soc. 2021;143(50):21127–21142. doi: 10.1021/jacs.1c10200.
[8] Phannaphat P, Pithalai P, Udomlak S, et al. Enhancement of antibacterial silk face covering with the biosynthesis of silver nanoparticles from *Garcinia mangostana Lin*n. Peel and Andrographis paniculata extract and a bacterial cellulose filter. Coatings. 2024;14(4):379. doi: 10.3390/coatings14040379.
[9] Abdussalam-Mohammed W. Comparison of chemical and biological properties of metal nanoparticles (Au, Ag) with metal oxide nanoparticles (ZnO-NPs) and their applications. Adv J Chem A. 2020;3(2):192–210. doi: 10.33945/SAMI/AJCA.2020.2.8.
[10] Nithya M, Ragavendran C, Natarajan D. Antibacterial and free radical scavenging activity of a medicinal plant *Solanum xanthocarpum*. Int J Food Prop. 2018;21(1):313–327. doi: 10.1080/10942912.2017.1409236.
[11] Bharathi D, Lee J, Karthiga P, et al. Kiwi fruit peel biowaste mediated green synthesis of silver nanoparticles for enhanced dye degradation and antibacterial activity. Waste Biomass Valor. 2024;15(3):1859–1868. doi: 10.1007/s12649-023-02328-9.
[12] Ahmad F, Ashraf N, Ashraf T, et al. Biological synthesis of metallic nanoparticles (MNPs) by plants and microbes: their cellular uptake, biocompatibility, and biomedical applications. Appl Microbiol Biotechnol. 2019;103(7):2913–2935. doi: 10.1007/s00253-019-09675-5.
[13] Marslin G, Siram K, Maqbool Q, et al. Secondary metabolites in the green synthesis of metallic nanoparticles. Materials. 2018;11(6):940. doi: 10.3390/ma11060940.
[14] Hawadak J, Kojom Foko LP, Pande V, et al. *In vitro* antiplasmodial activity, hemocompatibility and temporal stability of *Azadirachta indica* silver nanoparticles. Artif Cells Nanomed Biotechnol. 2022;50(1):286–300. doi: 10.1080/21691401.2022.2126979.
[15] Mohiuddin A, Saha MK, Hossian MS, et al. Usefulness of banana (*Musa paradisiaca*) wastes in manufacturing of bio-products: a review. Agriculturists. 2014;12(1):148–158. doi: 10.3329/agric.v12i1.19870.
[16] Aritonang HF, Koleangan H, Wuntu AD. Synthesis of silver nanoparticles using aqueous extract of medicinal plants' (*Impatiens balsamina* and *Lantana camara*) fresh leaves and analysis of antimicrobial activity. Int J Microbiol. 2019;2019:8642303–8642308. doi: 10.1155/2019/8642303.
[17] Maruthai J, Muthukumarasamy A, Baskaran B. Fabrication and characterisation of silver nanoparticles using bract extract of *Musa paradisiaca* for its synergistic combating effect on phytopathogens, free radical scavenging activity, and catalytic efficiency. IET Nanobiotechnol. 2019;13(2):134–143. doi: 10.1049/iet-nbt.2018.5136.
[18] Suresh J, Pradheesh G, Alexramani V, et al. Phytochemical screening, characterization and antimicrobial, anticancer activity of biosynthesized zinc oxide nanoparticles using cyathea nilgiriensis holttum plant extract. J Bionanosci. 2018;12(1):37–48. doi: 10.1166/jbns.2018.1494.
[19] Ii GVW, Kerscher P, Brown RM, et al. Green Synthesis of Robust, Biocompatible Silver Nanoparticles Using Garlic Extract. J Nanomater. 2012:2012:730746. doi: 10.1155/2012/730746.
[20] Jain S, Mehata MS. Medicinal plant leaf extract and pure flavonoid mediated green synthesis of silver nanoparticles and their enhanced antibacterial property. Sci Rep. 2017;7(1):1–13. doi: 10.1038/s41598-017-15724-8.

[21] Mat Yusuf SNA, Che Mood CNA, Ahmad NH, et al. Optimization of biogenic synthesis of silver nanoparticles from flavonoid-rich *Clinacanthus nutans* leaf and stem aqueous extracts. R Soc Open Sci. 2020;7(7):200065. doi: 10.1098/rsos.200065.

[22] Tomaszewska E, Soliwoda K, Kadziola K, et al. Detection limits of DLS and UV-Vis spectroscopy in characterization of polydisperse nanoparticles colloids. J Nanomater. 2013;2013(1):313081. doi: 10.1155/2013/313081.

[23] Netala VR, Bethu MS, Pushpalatha B, et al. Biogenesis of silver nanoparticles using endophytic fungus Pestalotiopsis microspora and evaluation of their antioxidant and anticancer activities. Int J Nanomedicine. 2016;11:5683–5696. doi: 10.2147/IJN.S112857.

[24] Wagner H, Bauer R, Melchart D, et al. Chromatographic Fingerprint Analysis of Herbal Medicines Thin-layer and High Performance Liquid. Wien, New York: Springer; 2011.

[25] Naeim H, El-Hawiet A, Abdel Rahman RA, et al. Antibacterial activity of *Centaurea pumilio* L. Root and aerial part extracts against some multidrug resistant bacteria. BMC Complement Med Ther. 2020;20(1):79. doi: 10.1186/s12906-020-2876-y.

[26] Zarei M, Jamnejad A, Khajehali E. Antibacterial effect of silver nanoparticles against four foodborne pathogens. Jundishapur J Microbiol. 2014;7(1):e8720. doi: 10.5812/jjm.8720.

[27] Mariscal A, Lopez-Gigosos RM, Carnero-Varo M, et al. Fluorescent assay based on resazurin for detection of activity of disinfectants against bacterial biofilm. Appl Microbiol Biotechnol. 2009;82(4):773–783. doi: 10.1007/s00253-009-1879-x.

[28] Devanesan S, AlSalhi MS, Balaji RV, et al. Antimicrobial and cytotoxicity effects of synthesized silver nanoparticles from *Punica granatum* peel extract. Nanoscale Res Lett. 2018;13(1):315. doi: 10.1186/s11671-018-2731-y.

[29] Singh H, Du J, Singh P, et al. Ecofriendly synthesis of silver and gold nanoparticles by *Euphrasia officinalis* leaf extract and its biomedical applications. Artif Cells Nanomed Biotechnol. 2018;46(6):1163–1170. doi: 10.1080/21691401.2017.1362417.

[30] Zayra G, Oliveira S, Afonso C, et al. Synthesis of silver nanoparticles using aqueous extracts of *Pterodon emarginatus* leaves collected in the summer and winter seasons. Int Nano Lett. 2019;9(2):109–117. doi: 10.1007/s40089-019-0265-7.

[31] Guzmán MG, Dille J, Godet S. Synthesis of silver nanoparticles by chemical reduction method and their antibacterial activity. Int J Chem Biomol Eng. 2009;2(3):104–111.

[32] Tripathy A, Raichur AM, Chandrasekaran N, et al. Process variables in biomimetic synthesis of silver nanoparticles by aqueous extract of *Azadirachta indica* (Neem) leaves. J Nanopart Res. 2010;12(1):237–246. doi: 10.1007/s11051-009-9602-5.

[33] Albanese A, Tang PS, Chan WCW. The effect of nanoparticle size, shape, and surface chemistry on biological systems. Annu Rev Biomed Eng. 2012;14(1):1–16. doi: 10.1146/annurev-bioeng-071811-150124.

[34] Menichetti A, Mavridi-Printezi A, Mordini D, et al. Effect of size, shape and surface functionalization on the antibacterial activity of silver nanoparticles. J Funct Biomater. 2023;14(5):244. doi: 10.3390/jfb14050244.

[35] Le Ouay B, Stellacci F. Antibacterial activity of silver nanoparticles: a surface science insight. Nano Today. 2015;10(3):339–354. doi: 10.1016/j.nantod.2015.04.002.

[36] Siakavella IK, Lamari F, Papoulis D, et al. Effect of plant extracts on the characteristics of silver nanoparticles for topical application. Pharmaceutics. 2020;12(12):1244. doi: 10.3390/pharmaceutics12121244.

[37] Gangadhar S, Vilas V, Rokade AA, et al. Green synthesis and characterization of silver nanoparticles (Ag NPs) from extract of plant Radix Puerariae: an efficient and recyclable catalyst for the construction of pyrimido [1, 2-b] indazole derivatives under solvent-free conditions. Catal Commun. 2017;99(June):121–126. doi: 10.1016/j.catcom.2017.06.006.

[38] Xu Z, Zha X, Ji R, et al. Green biosynthesis of silver nanoparticles using aqueous extracts of *Ageratum conyzoides* and their anti-inflammatory effects. ACS Appl Mater Interfaces. 2023;15(11):13983–13992. doi: 10.1021/acsami.2c22114.

[39] Hoo CM, Starostin N, West P, et al. A comparison of atomic force microscopy (AFM) and dynamic light scattering (DLS) methods to characterize nanoparticle size distributions. J Nanopart Res. 2008;10(S1):89–96. doi: 10.1007/s11051-008-9435-7.

[40] Matlou GG, Managa M, Nyokong T. Effect of symmetry and metal nanoparticles on the photophysicochemical and photodynamic therapy properties of cinnamic acid zinc phthalocyanine. Spectrochim Acta A Mol Biomol Spectrosc. 2019;214:49–57. doi: 10.1016/j.saa.2019.02.005.

[41] Gu F, Hu C, Tai Z, et al. Tumour microenvironment-responsive lipoic acid nanoparticles for targeted delivery of docetaxel to lung cancer. Sci Rep. 2016;6(1):36281. doi: 10.1038/srep36281.

[42] Martínez-Cabanas M, López-García M, Rodríguez-Barro P, et al. Antioxidant capacity assessment of plant extracts for green synthesis of nanoparticles. Nanomaterials. 2021;11(7):1679. doi: 10.3390/nano11071679.

[43] Wypij M, Jędrzejewski T, Trzcińska-Wencel J, et al. Green synthesized silver nanoparticles: antibacterial and anticancer activities, biocompatibility, and analyses of surface-attached proteins. Front Microbiol. 2021;12(April):632505. doi: 10.3389/fmicb.2021.632505.

[44] Ahmad A, Wei Y, Syed F, et al. The effects of bacteria-nanoparticles interface on the antibacterial activity of green synthesized silver nanoparticles. Microb Pathog. 2017;102(2017):133–142. doi: 10.1016/j.micpath.2016.11.030.

[45] Prem P, Naveenkumar S, Kamaraj C, et al. *Valeriana jatamansi* root extract a potent source for biosynthesis of silver nanoparticles and their biomedical applications, and photocatalytic decomposition. Green Chem Lett Rev. 2024. 17(1):2305142. doi: 10.1080/17518253.2024.2305142.

[46] Erno P, Philippe B, Martin B. Structure determination of organic compounds: tables of spectral data. 4th edition. Germany: Springer; 2018. doi: 10.1007/978-3-540-93810-1.

[47] Kumar Sur U, Ankamwar B, Karmakar S, et al. Green synthesis of Silver nanoparticles using the plant extract of Shikakai and Reetha. Mater Today: Proc. 2018;5(1):2321–2329. doi: 10.1016/j.matpr.2017.09.236.

[48] Shah Z, Hassan S, Shaheen K, et al. Synthesis of AgNPs coated with secondary metabolites of *Acacia nilotica*: an efficient antimicrobial and detoxification agent for environmental toxic organic pollutants. Mater Sci Eng C Mater Biol Appl. 2020;111(February):110829. doi: 10.1016/j.msec.2020.110829.

[49] Sherin L, Sohail A, Amjad UeS, et al. Facile green synthesis of silver nanoparticles using *Terminalia bellerica* kernel extract for catalytic reduction of anthropogenic water pollutants. Colloids Interface Sci Commun. 2020;37(May):100276. doi: 10.1016/j.colcom.2020.100276.

[50] Ahmed A, Rauf A, Hemeg HA, et al. Green synthesis of gold and silver nanoparticles using opuntia dillenii aqueous extracts: characterization and their antimicrobial assessment. J Nanomater. 2022;2022(1):4804116. doi: 10.1155/2022/4804116.

[51] Pereira TM, Polez VLP, Sousa MH, et al. Modulating physical, chemical, and biological properties of silver nanoparticles obtained by green synthesis using different parts of the tree *Handroanthus heptaphyllus* (Vell.) Mattos. Colloids Interface Sci Commun. 2020;34(December 2019):100224. doi: 10.1016/j.colcom.2019.100224.

[52] Kambale EK, Nkanga CI, Mutonkole BPI, et al. Green synthesis of antimicrobial silver nanoparticles using aqueous leaf extracts from three Congolese plant species (*Brillantaisia patula*, *Crossopteryx febrifuga* and *Senna siamea*). Heliyon. 2020;6(8):e04493. doi: 10.1016/j.heliyon.2020.e04493.

[53] Oyeyinka BO, Afolayan AJ. Comparative and correlational evaluation of the phytochemical constituents and antioxidant activity

of *Musa sinensis* L. and *Musa paradisiaca* L. Fruit Compartments (Musaceae). ScientificWorldJournal. 2020;2020:4503824–4503812. doi: 10.1155/2020/4503824.

[54] Fathima A, Rao JR. Selective toxicity of Catechin—a natural flavonoid towards bacteria. Appl Microbiol Biotechnol. 2016;100(14):6395–6402. doi: 10.1007/s00253-016-7492-x.

[55] Reygaert WC. The antimicrobial possibilities of green tea. Front Microbiol. 2014;5:434. doi: 10.3389/fmicb.2014.00434.

[56] Sre NZ, Nedi ZP, Monti DM, et al. Biosynthesis of silver nanoparticles using *Salvia pratensis* L. aerial part and root extracts: bioactivity, biocompatibility, and catalytic Potential. Molecules. 2023;28(3):1387. doi: 10.3390/molecules28031387.